

# Experimental Evaluation of the High Performance Vector Controlled Matrix Converter-Fed Induction Motor

UDK 621.33.07  
IFAC IA 5.5.4;4.0.1

Original scientific paper

The results of the intensive experimental study of the matrix converter-fed Induction Motors (IM) with high dynamic performance speed-flux tracking field-oriented control algorithm are presented. It is experimentally proven that high performance speed tracking is achieved under heavy dynamic conditions of operation. High quality input/output current waveforms of the matrix converter obtained during steady state conditions of operations for both directions of the power flow. The results of the experimental tests prove that matrix converter does not have limitations for implementation in high dynamic performance vector controlled induction motor drives.

**Key words:** commutation strategy, induction motors, matrix converter, space vector modulation, vector control

## 1 INTRODUCTION

Electromechanical energy conversion using different kinds of electric motors is one of the most important areas of applications for modern semiconductor power converters. Recent requirements for power converters to be implemented in high performance electrical drives include:

- high precision tracking of the reference voltage vector;
- bi-directional power flow capability;
- controlled input power factor;
- matching of the electromagnetic compatibility requirements.

At present time these requirements can be achieved using two types of power converters: standard AC-DC-AC converters with vector controlled input rectifier and direct frequency converters known as matrix converters (MC). Back-to-back AC-DC-AC converters have been intensively studied [1] and now they established the industrial standard for medium and high power applications. Recently matrix converters have been found as attractive alternative to AC-DC-AC converters [2].

Number of promising results on application of MC for control in electromechanical systems are reported in literature: IM drives [3], synchronous motor drives [4], doubly-fed induction machine [5, 6]. Nevertheless as far as authors know MC never has been tested in heavy dynamic conditions of operation, which are typical for vector controlled IM drives.

In this paper we present results of intensive experimental study of the high dynamic performance vector controlled induction motor fed by MC. For

both MC and IM control we use recently developed by authors novel control algorithms.

An improved direct field-oriented control algorithm for IM [7] with speed-flux tracking capabilities has been selected for evaluation of the MC performance, since it requires the high precision tracking of the reference voltage vector during heavy dynamic conditions. A new space vector modulation (SVM) and improved commutation strategy have been implemented for matrix converter control [8]. The main features of the proposed SVM control are: linear loading of the line source (MC is viewed by the line source as linear load); high precision tracking of the reference voltage vector. No information about output current direction and relation between input phase voltages are required for implementation of the MC commutation.

The main conclusions from the results of experimental study can be summarized as follows: i) matrix converter control algorithms provide high precision voltage tracking suitable for implementation in high dynamic performance AC electrical drives; ii) safe commutation of the MC switching is achieved in all condition of IM operation without of detection of the output current direction; iii) the satisfactory waveforms of the input and output currents are observed from the tests.

The paper is organized as follows. In Section II the short description of MC control algorithm is given. Section III presents general configuration of improved vector control algorithm for IM. Results of experimental testing of the MC during steady state and during vector control of the IM are given in Section IV.

### 2 MATRIX CONVERTER CONTROL

Figure 1 shows the matrix converter topology, connecting the 3 input lines to 3 output lines with help of nine bi-directional IGBT-switches S1-S9. The SVM control technique of MC is based on the instantaneous space-vector representation of output voltage and input current.

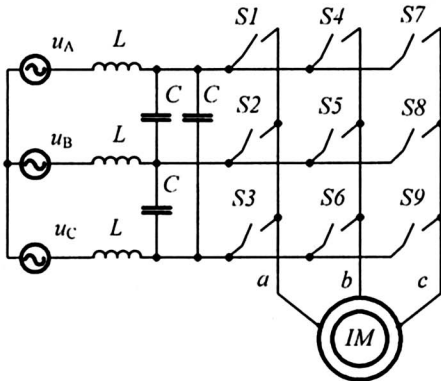


Fig. 1 Matrix converter topology

The averaged values of the reference voltage vector  $\mathbf{u}_{ref}$  are obtained as the result of synthesis from the five stationary vectors (four non-zero and one zero) [2, 9, 10]. The desired averaged phase voltage  $\mathbf{u}_{ref}$  in each of six sectors (Figure 2a) is defined as follows:

$$\mathbf{u}_{ref} = \sqrt{u_a^2 + u_b^2} e^{j\theta_o(t)} = \sum_{k=1}^4 d_k \mathbf{u}_{ok} \quad (1)$$

where  $\mathbf{u}_{ok}$  are the non-zero stationary vectors;  $d_k$  is on-time ratio;  $d_k = t_k/T_M$ ;  $t_k$  is the interval duration, in which  $\mathbf{u}_{ok}$  vectors are acting during current SVM period  $T_M$ ;  $u_a$  and  $u_b$  are the components of  $\mathbf{u}_{ref}$  in orthogonal coordinate system a-b,  $\theta_0$  is a instantaneous angle of the space output voltage vectors with respect to its initial position in the sector under consideration, Figure 2a.

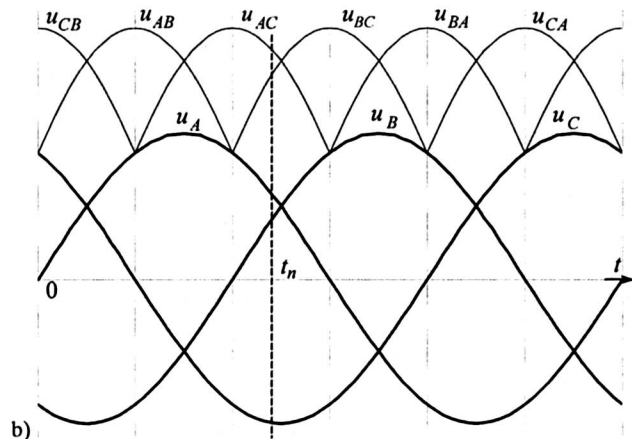
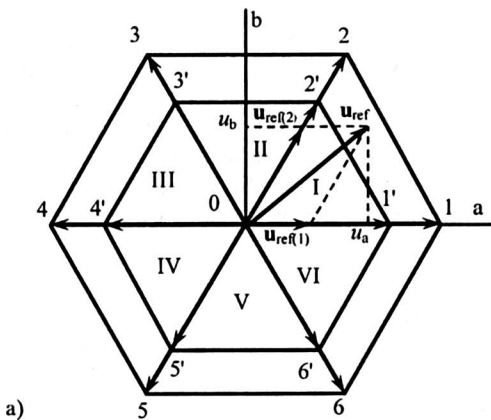


Fig. 2 Output space voltage vector diagram (a). Input voltages time diagram (b)

Let us consider the case, when there are no shift between the input current and voltage vectors. In order to form the non-zero vectors the two input line-to-line voltages with maximum instantaneous values are alternatively used. Zero vector is formed when all output phases are turned on to the same input phase. The basis of the proposed SVM is the argument that AC mains, feeding the MC, should be linearly loaded [9]. In this case the waveform of the averaged MC input current is sinusoidal under sinusoidal input voltage conditions. Two input line to-line voltages are selected in each of six 60-degrees intervals, the boundaries of which are determined by the transition moments of any phase voltage wave through zero, Figure 2b. Inside these intervals the two phase voltages have identical polarity and the third one with maximum instantaneous value has opposite polarity. Correspondingly, the third phase is involved during all SVM cycles and the first two phases alternately. The input current running in the third phase is distributed between the two other phases according to SVM law.

Let us discourage the two input phases which have the same voltage polarities inside of the 60-degrees intervals as  $\delta$  and  $\gamma$  and the third phase with opposite voltage polarity by index  $\nu$ . For example at the instant of time  $t_n$  under consideration in Figure 2b  $u_\delta = u_A$ ,  $u_\gamma = u_B$ ,  $u_\nu = u_C$ . For other 60-degrees intervals the indexes will be transposed according to the rule above.

In order to provide the linear loading of AC input the following proportion should be satisfied [9]

$$\frac{d_\delta}{d_\gamma} = \frac{u_\delta}{u_\gamma} \quad (2)$$

where  $d_\delta$  and  $d_\gamma$  are on-time ratios for phases  $\delta$  and  $\gamma$  respectively.

Define the components of the output voltage space vector  $\mathbf{u}_{ref}$  oriented along directions of the vectors, forming the sector in which vector  $\mathbf{u}_{ref}$  is allocated, as  $\mathbf{u}_{ref(n)}$  ( $n=1\dots6$ ), Figure 2a (the right boundary of the  $n^{\text{th}}$  sector corresponds to the  $\mathbf{u}_{ref(n)}$ ). The amplitude of each component for considered sectors of input phases is equal to

$$\begin{aligned} |\mathbf{u}_{ref(n)}| &= \frac{2}{3} |d_{\delta(n)}u_{\delta v} + d_{\gamma(n)}u_{\gamma v}| = \\ &= \frac{2}{3} |d_{\delta(n)}(u_{\delta} - u_v) + d_{\gamma(n)}(u_{\gamma} - u_v)| \end{aligned} \quad (3)$$

where  $d_{\delta(n)}$  and  $d_{\gamma(n)}$  are on-time ratios for phases  $\delta$  and  $\gamma$  respectively.

Taking into account (2) the expression (3) becomes

$$|\mathbf{u}_{ref(n)}| = \frac{2}{3} d_{\delta(n)} \frac{\Delta}{|u_{\delta}|} = \frac{2}{3} d_{\gamma(n)} \frac{\Delta}{|u_{\gamma}|} \quad (4)$$

where  $\Delta = u_{\delta}^2 + u_{\gamma}^2 - (u_{\delta} + u_{\gamma})u_v$ .

Note that if the sum of instantaneous values of the phase voltages is equal to zero, then

$$\Delta = u_{\delta}^2 + u_{\gamma}^2 + u_v^2 = u_A^2 + u_B^2 + u_C^2.$$

If MC is fed from a symmetrical voltage system then  $\Delta = (3/2)U_{mi}^2$  where  $U_{mi}$  is the input phase voltage amplitude.

When components  $\mathbf{u}_{ref(n)}$  of the  $\mathbf{u}_{ref}$  are considered in a-b coordinate frame then from (4) we have

$$\begin{bmatrix} d_{\delta(n)} \\ d_{\gamma(n)} \\ d_{\delta(n+1)} \\ d_{\gamma(n+1)} \end{bmatrix} = \frac{\sqrt{3}}{\Delta} \begin{bmatrix} |u_{\delta}| \left( u_a \sin \frac{n\pi}{3} - u_b \cos \frac{n\pi}{3} \right) \\ |u_{\gamma}| \left( u_a \sin \frac{n\pi}{3} - u_b \cos \frac{n\pi}{3} \right) \\ |u_{\delta}| \left( -u_a \sin \frac{(n-1)\pi}{3} + u_b \cos \frac{(n-1)\pi}{3} \right) \\ |u_{\gamma}| \left( -u_a \sin \frac{(n-1)\pi}{3} + u_b \cos \frac{(n-1)\pi}{3} \right) \end{bmatrix}. \quad (5)$$

The on-time ratio for zero vector is equal to

$$d_0 = 1 - d_{\delta(n)} - d_{\gamma(n)} - d_{\delta(n+1)} - d_{\gamma(n+1)}.$$

With the such forming of the SVM the following features are obtained:

- linear loading of the symmetrical line source (MC is viewed by the line source as linear load);
- high precision tracking of the reference voltage vector  $\mathbf{u}_{ref}$  under deviations of input voltages and the unbalanced voltage supply system.

The commutation strategy in MC can be based on two approaches. The first, based on the current direction information and the second, based on measured AC input phase voltages relationship [2]. In this work a novel mode is used. As compared with the other approaches it requires no detection of the current direction and measurement of the relation of input voltage values, but only the detection of their polarity.

The proposed step-by-step commutation strategy of transistors excludes the current commutation by the switches, connected to the mains phases, whose voltage curves are crossed inside of the current time interval (Figure 2b). This approach is realized by means of the optimal choice the order for forming of the stationary vectors in time and by special method of forming of zero vectors, consisting in simultaneous switching on all the switches, connected to the mains phase with maximum voltage modulus during current time interval.

Figure 3a shows the stationary vectors, denoted as  $\delta\alpha$ ,  $\delta\beta$  (being formed from line voltage  $\pm u_{\delta v}$ ),  $\gamma\alpha$ ,  $\gamma\beta$  (being formed from line voltage  $\pm u_{\gamma v}$ ) and  $\mathbf{0}$  (zero vector). The reference line-to-neutral voltage vector  $\mathbf{u}_{ref}$  is supposed to be placed inside sector, formed by above mentioned vectors.

The dashed lines in Figure 3a show the vectors alternation which guarantees the safe step-by-step commutations. Such groups of vectors are  $\mathbf{0}$ ,  $\delta\alpha$ ,  $\delta\beta$  and  $\mathbf{0}$ ,  $\gamma\alpha$ ,  $\gamma\beta$ .

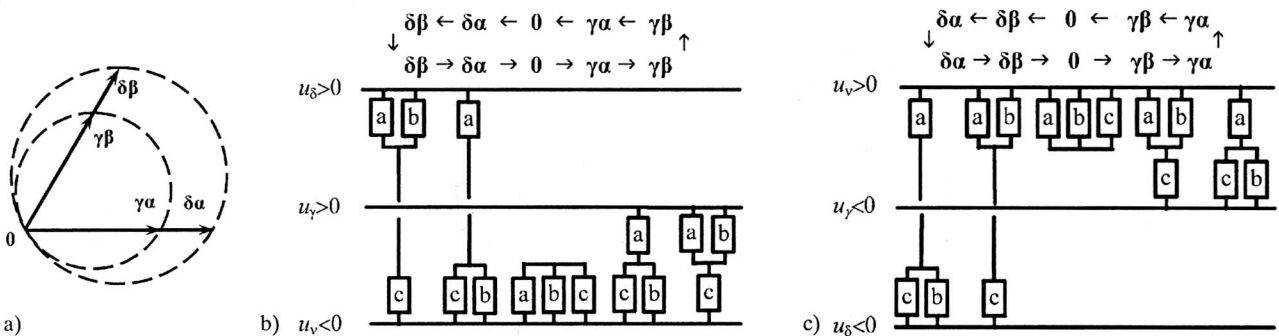


Fig. 3 Alternation of vectors (a). Sequence of commutations under  $u_v < 0$  (b) and  $u_v > 0$  (c)

Figures 3.b and 3.c correspond for two cases, when  $u_v < 0$  and  $u_v > 0$ . They illustrate the sequence of commutations in single SVM cycle, transition to the next cycle and the configurations of the load phases a, b, c, corresponding to each stationary vector, if vector  $\mathbf{u}_{ref}$  is placed, for example, in sector I (Figure 2.a). Presented version of switching algorithm guarantees the minimum number of commutations.

To implement the commutation strategy proposed the following steps are necessary:

- a) First the non-zero vectors of the one input line voltage are formed.
- b) Then the zero vector is formed.
- c) At the end of SVM cycle the non-zero vectors are constructed using other input line voltage.
- d) Under transition to the next SVM cycle both inside of sector and under movement of vector  $\mathbf{u}_{ref}$  from the one sector to another (Figure 2.a) first the non-zero vectors are placed. They are formed from the same line voltage used in forming of the last vector of the previous SVM cycle.

### 3 SPEED-FLUX TRACKING DIRECT FIELD-ORIENTED CONTROL ALGORITHM FOR IM

In order to test all control algorithms, proposed for MC, during heavy dynamic conditions closed to converter current and voltage limits we use recently developed by authors [7] new direct field-oriented vector control algorithm. Controller development is

based on novel design strategy for indirect field-orientation presented in [11]. This design approach has been modified in order to build observer-based output feedback controller based on stator currents and speed measurements. Specifically, the problem of flux-speed tracking with no singularities is addressed, in presence of unknown constant load torque and under the requirement of achieving new features for the closed loop dynamics:

- a) Global exponential asymptotic speed-flux tracking.
- b) Asymptotic speed-flux decoupling.
- c) Asymptotic linearization of the speed subsystem.
- d) Robustness with respect to IM parameter (especially rotor resistance) variations.

Following the same conceptual line as in [11] we design direct field-oriented controller with reduced order (second order), but closed loop flux observer. The two interconnected (electromechanical and electromagnetic) subsystems are designed, whose outputs are torque (speed) and flux vector, respectively, with the two transformed stator voltages responsible for control objectives in each subsystem. Based on the concept of field-oriented decomposition, special decoupling conditions are defined for speed and flux subsystems which allow to design an observer-based flux-vector control algorithm providing closed loop exponential asymptotic flux vector tracking as well as asymptotic speed-flux decoupling via asymptotic field orientation. The property of asymptotic linearization of the speed subsystem (even with time-varying flux level) allows to use of

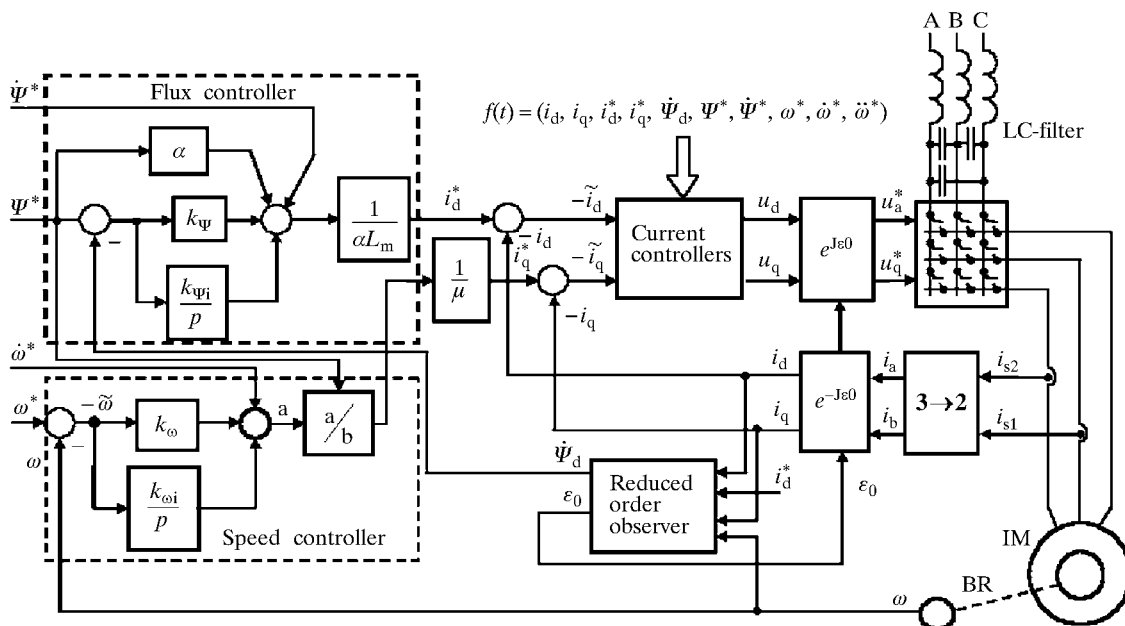


Fig. 4 Block-diagram of the vector controlled IM fed by MC

well-known linear optimization technique and speed controller parameters tuning procedure, commonly used in standard cascaded systems. Robustness of the speed subsystem is guaranteed by the two-level cascaded structure with astatic inner and outer loops having nonlinear current and speed controllers.

The flux subsystem is an open-loop system when the standard field-oriented control strategy with reduced order observer is used. This system is designed herein to get closed-loop properties. As result, significant improvement of the robustness with respect to rotor circuit parameters variation is achieved, when rotor speed is different from zero. The proposed observer-based flux controller is simpler as compared with controllers based on full order observers and does not require the information about stator voltages.

The block-diagram of the proposed system is shown in Figure 4. Structure of the current controllers in Figure 4 is the same as in [11] with the flux reference  $\Psi^*$  replaced by the estimated flux modulus  $\hat{\Psi}_d$ , given by the closed loop reduced order flux observer

$$\begin{aligned} \dot{\hat{\Psi}}_d &= -\alpha \hat{\Psi}_d + \alpha L_m i_d \\ \dot{\hat{\omega}}_0 &= \omega_0 = \omega p_n + \alpha L_m \frac{i_q}{\hat{\Psi}_d} + \frac{\gamma_1}{\hat{\Psi}_d} \omega \tilde{i}_d, \end{aligned} \quad (6)$$

where  $\alpha$  is inverse of rotor time constant,  $L_m$  – magnetizing inductance,  $p_n$  – number of pole pairs and  $\gamma_1 > 0$  is the tuning gain.

#### 4 EXPERIMENTAL TESTING OF THE MATRIX CONVERTER FED INDUCTION MACHINE

In order to justify the performance of the matrix converter and its implementability for high dynamic performance induction machine control an intensive

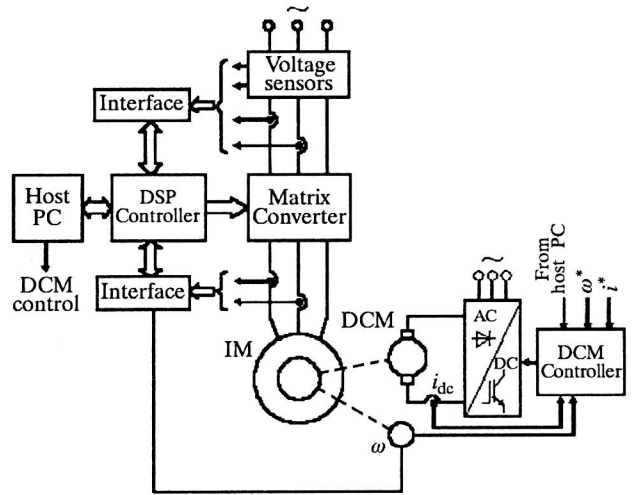


Fig. 5 Block diagram of the experimental set-up

experimental study have been performed. Our main interests of investigation have been concentrated on the evaluation of the dynamic capabilities of the MC during heavy dynamic conditions of operation, line current dynamics and availability to achieve zero speed induction machine operation when almost zero voltage of the MC is required.

#### 4.1 Experimental set-up

The experimental tests have been carried out using a Rapid Prototyping Station developed for testing the matrix converter fed electric machines. The Rapid Prototyping Station, whose block diagram shown in Figure 5, includes:

1. A wound rotor IM, whose rated data are listed in Appendix, supplied by MC. During investigation of vector controlled induction machine the IM rotor circuit is shortened.
2. A current controlled DC motor is used to provide the load torque for induction motor drive.

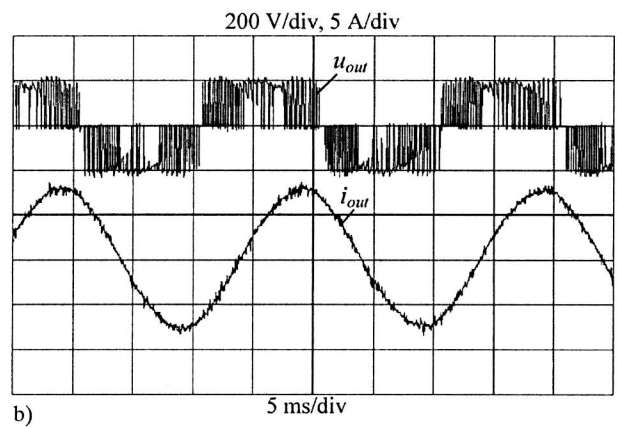
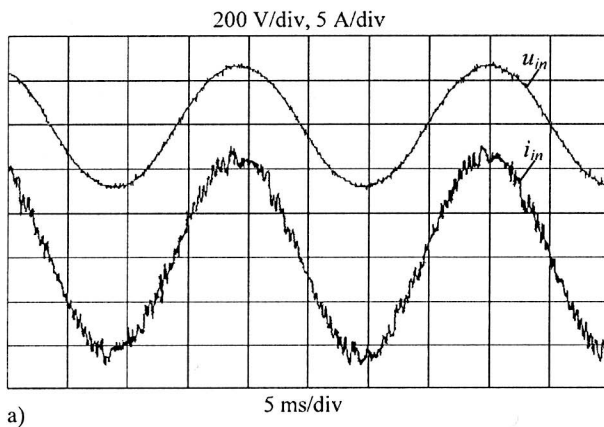


Fig. 6 Input voltage and input current (a). Output voltage and output current (b). Output frequency 50 Hz, carrier frequency 5 kHz

3. A 6 kVA matrix converter with input filter:  $L = 1$  mH,  $C = 10$   $\mu$ F.
4. A DSP-based real time controller implemented using »dSPACE DS1102« control board (TMS320C31) directly connected to PC bus. The sampling time for control implementation has been set at 200  $\mu$ s, the visualization and extended acquisition system of DS1102 were used for real time tracing of selected variables and data storage.
5. All analog signals have been measured using LEM current and voltage sensors and filtered with second order analog filters having cut-off frequency of 2 kHz. For speed and position measurements an incremental encoder with 5000 lines per revolution is used.
6. A personal computer acting as Operator Interface for programming, debugging, program downloading, virtual oscilloscope and automation function during the experiments.

Figure 6 shows the waveforms of MC input currents and voltages as well as output phase voltage and phase current during steady state operation of 1.4 kW induction motor with rated load.

#### 4.2 Vector controller tuning and implementation

The tuning parameters of the speed and flux subsystems are proportional and integral gains of the speed and flux controllers ( $k_{\omega}$ ,  $k_{\omega i}$ ,  $k_{\psi}$ ,  $k_{\psi i}$ ) as well as proportional and integral gains of the current controllers  $k_i$ ,  $k_{ii}$ . According to the structure of the cascaded system we use the standard tuning relation

$$k_i = \frac{k_p^2}{2} = \frac{1}{\tau^2}; \quad \xi = 0.707 \quad (7)$$

where  $\tau$  and  $\xi$  are the time constant and damping factor imposed for the second order error dynamics and  $k_p$ ,  $k_i$  are the proportional and integral gains in each loop. The time scale separation is achieved with  $\tau_s \geq (2-4)\tau_i$ , where indexes  $s$  and  $i$  stand for speed, flux and currents loops. To get the discrete time version of control algorithm the simple backward derivative (Euler) method is used. The controllers parameters, selected according to (7) were set at:  $k_{\omega} = 100$ ;  $k_{\omega i} = 5000$ ;  $k_i = 500$ ;  $k_{ii} = 125000$ ;  $k_{\psi} = 50$ ;  $k_{\psi i} = 1250$ .

All programs for controllers implementation have been written using C++ language.

#### Operating sequence

The operating sequences, reported in Figure 7, are the following:

1. The machine is exited during the initial time interval 0–0.25 s using a flux reference trajectory starting at  $\Psi^*(0) = 0.02$  Wb and reaching the motor rated value of 0.7 Wb with the first derivative equal to 2.72 Wb/s.
2. The unloaded motor is required to track the speed reference trajectory, starting at time  $t = 0.5$  s from zero initial value and reaching the speed of 50 rad/s (60 % of rated) with the first and second derivatives equal to 420 rad/s<sup>2</sup> and 8239 rad/s<sup>3</sup>.
3. During time interval of constant speed rotation the step load torque, equal to rated value, is applied and removed.
4. The final time interval is given for unloaded motor braking to zero speed.

Tracking of the speed reference trajectory adopted requires a dynamic torque, which is equal to double of rated value of the IM.

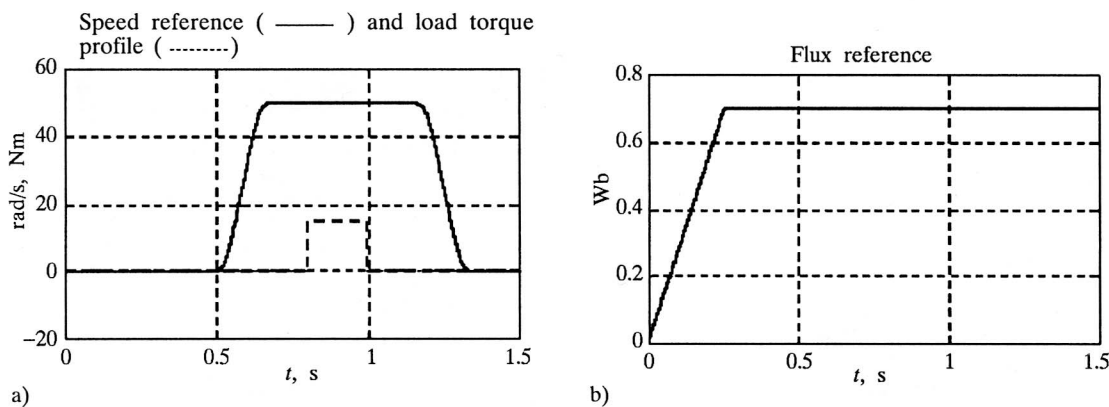


Fig. 7 Speed, flux references and load torque profile

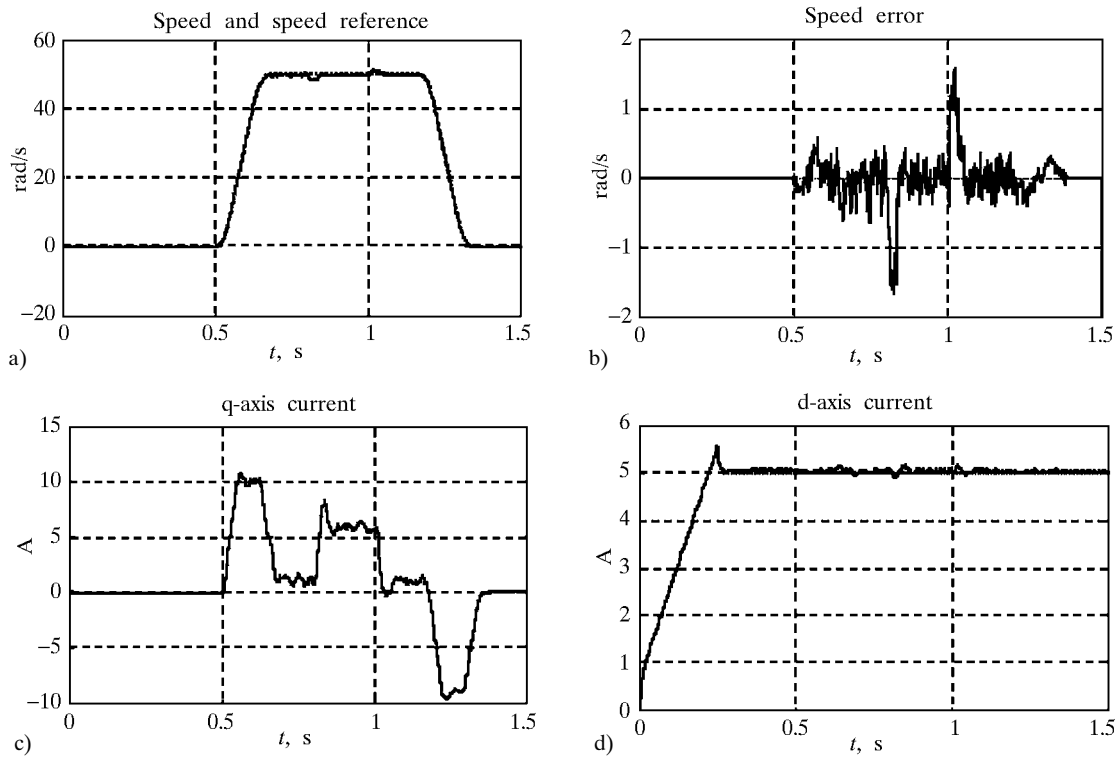


Fig. 8 Transient performance of the proposed controller

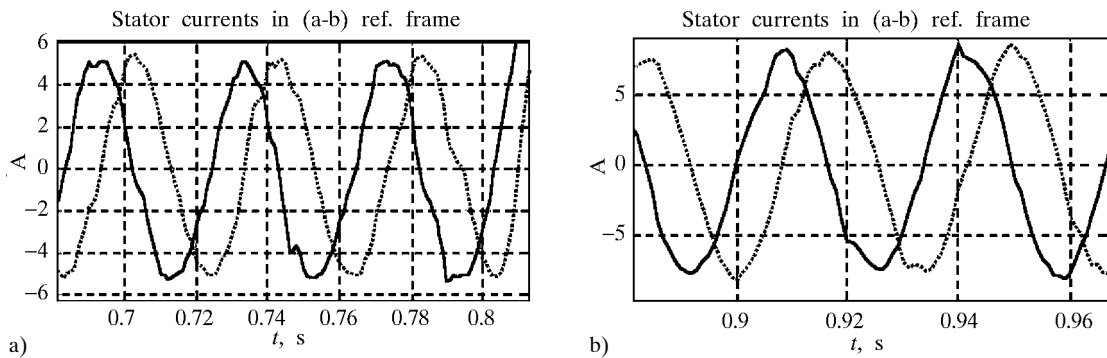


Fig. 9 Stator currents waveforms during steady state condition  $\omega = 50$  rad/s: (a) no load torque; (b) rated load torque

**4.3 Experimental results of vector controlled IM**

The experimental results presented in Figure 8 demonstrate the dynamic performance of the proposed controller adopting the controller tuning according to (7). The speed tracking performance (maximum speed error of about 0.3 rad/s) satisfied the requirements of any high dynamic performance applications. The Figures 9.a and 9.b demonstrate the waveforms of the stator current during steady state condition  $\omega = 50$  rad/s without load and with rated load.

The operation near by zero speed with  $\omega^* = 0.05$  rad/s is shown in Figure 10. Excellent steady state

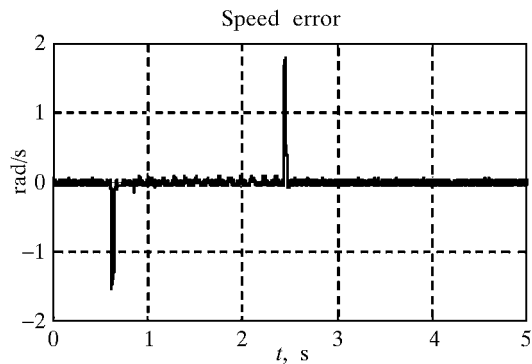


Fig. 10 Operation near by zero speed:  $\omega^* = 0.05$  rad/s, rated load is applied at  $t = 0.6$  s and removed at  $t = 2.4$  s

performance and dynamics during load torque rejection is achieved during this regime of operation in low MC voltage region.

## 5 CONCLUSIONS

It is experimentally demonstrated that performance of the investigated MC-fed vector controlled induction motor has no significant difference with that of standard AC-DC-AC converter-fed configurations. From intensive experimental study we conclude that proposed solutions for matrix converter control and control algorithms for matrix converter fed IMs are suitable for any high dynamic performance applications.

## APPENDIX

Rated power	1.4 kW
Rated current	5.2 A
Rated voltage	380 V
Rated torque	15 Nm
Rated speed	880 rev/min
Number of pole pair	$p_n = 3$
Rotor resistance	$R_2 = 5.3 \Omega$
Stator resistance	$R_1 = 4.7 \Omega$
Stator inductance	$L_1 = 0.161 \text{ H}$
Rotor inductance	$L_2 = 0.161 \text{ H}$
Mutual inductance	$L_m = 0.138 \text{ H}$
Viscous friction coefficient	$\nu = 0.45$

**Eksperimentalna provjera vektorski upravljano g asinkronog motora visokih performanci napajano g iz matričnog pretvarača.** U članku se izlažu rezultati temeljite eksperimentalne studije o asinkronom motoru napajanom iz matričnog pretvarača i upravljano m prema načelu vektorske regulacije s visokim dinamičkim performansama slijeđenja referencije brzine vrtnje i magnetskog toka. Eksperimentom je pokazano da se visoke performance slijeđenja brzine vrtnje postižu u uvjetima teškog dinamičkog opterećenja motora. Dobivena je visoka kvaliteta valnih oblika ulazne i izlazne struje matričnog pretvarača za stacionarno stanje i za oba smjera toka energije. Rezultati eksperimentalnog ispitivanja potvrđuju da ne postoje ograničenja na primjenu matričnog pretvarača u vektorski upravljanim asinkronim pogonima visokih dinamičkih svojstava.

**Ključne riječi:** matrični pretvarač, asinkroni motor, vektorska modulacija, strategija komunikacije, vektorsko upravljanje

## REFERENCES

- [1] B. K. Bose, **Power Electronics and Variable Frequency Drives: Technology and Applications**. IEEE Press, N.Y., 1996.
- [2] P. Wheeler, D. Grant, **Matrix Converter Technology**. EPE'99, – Tutorial, Lausanne, Switzerland, 1999.
- [3] S. Sunter, J. C. Clare, **A True Four Quadrant Matrix Converter Induction Motor Drive with Servo Performance**. IEEE Power Electronics Specialists Conference, Italy, pp. 146–151, May 1996.
- [4] Bouchiker Said, G.-A. Capolino, M. Poloujadoff, **Vector Control of a Permanent-Magnet Synchronous Motor Using AC-AC Matrix Converter**. IEEE Trans. Power Electronics, Vol. 13, no. 6, pp. 1089–1099, 1998.
- [5] L. Zhang, C. Watthanasarn, W. Shepherd, **Application of a Matrix Converter for the Power Control of a Variable-Speed Wind-Turbine Driving a Doubly-Fed Induction Generator**. Proc. IECON97, Vol. 2, pp. 906–911, 1997.
- [6] E. Chekhet, S. Peresada, V. Sobolev, **Novel Vector Control Algorithm of the Doubly Fed Induction Machine with Matrix Converter**. Proc. PEMC'98, Prague, Czech. Republic, Vol. 5, pp. 5.123–5.128, 1998.
- [7] S. Peresada, S. Kovbasa, E. Chekhet, I. Shapoval, **High Performance Electromechanical Energy Conversion Using Matrix Converter**. Part 2: Vector Control of Induction Motor. Proc. of Intern. Conf. »Problems of Electrical Drives«, Alushta, Ukraine, pp. 263–266, 2001.
- [8] E. Chekhet, V. Mikhalsky, V. Sobolev, I. Shapoval, **Control Technique for Matrix Converter**. Proc. of the 5<sup>th</sup> Conf. UEES' 2001, Szczecin, Poland, Vol. 2, pp. 583–588, 2001.
- [9] E. Chekhet, D. Izosimov, T. Misak, **Space Vector Pulse-width Modulation in Direct Frequency Converters**. Proc. PEMC'94, Warsaw. Poland, pp. 468–473, 1994.
- [10] L. Zhang, C. Watthanasarn, W. Shephard, **Analysis and Implementation of a Space Vector Modulation Algorithm for Direct ac-ac Matrix Converters**. EPE Journal, Vol. 6, no. 1, pp. 284–284, May 1996.
- [11] S. Peresada, A. Tonielli, **High-performance Robust Speed-flux Tracking Controller for Induction Motor**. International Journal of adaptive control and signal processing, Vol. 14, no. 2–3, pp. 177–200, 2000.

## AUTHORS' ADDRESSES:

Eduard Chekhet  
Sergej Peresada\*  
Vladimir Sobolev  
Valery Mikhalsky  
Sergej Kovbasa\*

Institute of Electrodynamics of the Ukrainian National Academy of Sciences, Prospect Pobedy 56, 03680, Kiev, Ukraine  
Tel/Fax: (+38 044) 456 92 66, e-mail: chk@ied.kiev.ua

\* National Technical University of Ukraine »Kiev Polytechnical Institute«, Prospect Pobedy 37, 252056, Kiev, Ukraine  
Tel: (+38 044) 264 58 36, e-mail: peresada@i.com.ua

Received: 2003–10–20